Crystal structure of edoxaban tosylate monohydrate Form I, ($C_{24}H_{31}ClN_7O_4S$)($C_7H_7O_3S$)(H_2O)

James A. Kaduk,[1,2,a)] Amy M. Gindhart,[3] and Thomas N. Blanton[3]
[1]North Central College, 131 S. Loomis St., Naperville, Illinois 60540, USA
[2]Illinois Institute of Technology, 3101 S. Dearborn St., Chicago, Illinois 60616, USA
[3]ICDD, 12 Campus Blvd., Newtown Square, Pennsylvania 19073-3273, USA

(Received 18 November 2020; accepted 15 January 2021)

The crystal structure of edoxaban tosylate monohydrate has been solved and refined using synchrotron X-ray powder diffraction data, and optimized using density functional techniques. Edoxaban tosylate monohydrate crystallizes in space group $P2_1$ (#4) with $a = 7.55097(2)$, $b = 7.09010(2)$, $c = 32.80420(21)$ Å, $\beta = 96.6720(3)°$, $V = 1744.348(6)$ Å^3, and $Z = 2$. The crystal structure consists of alternating layers of edoxaban cations and tosylate anions along the *c*-axis. The water molecules lie near the sulfonate end of the tosylate anions. The solid-state conformation of the edoxaban cation is determined by intermolecular interactions. The protonated nitrogen atom forms a strong N–H···O hydrogen bond to one of the tosylate oxygens. Only one of the water molecule hydrogens acts as a donor in an O–H···O hydrogen bond. The tosylate oxygens act as acceptors in a number of C–H···O hydrogen bonds. The powder pattern has been submitted to ICDD® for inclusion in the Powder Diffraction File™. © *The Author(s), 2021. Published by Cambridge University Press on behalf of International Centre for Diffraction Data.*
[doi:10.1017/S0885715621000117]

Key words: edoxaban, Lixiana®, Rietveld refinement, density functional theory

I. INTRODUCTION

Edoxaban tosylate monohydrate is an anticoagulant (under the brand names Lixiana®, Savaysa®, and others), used for treatment of deep vein thrombosis and pulmonary embolism. It functions as an anticoagulant, a coagulant factor Xa inhibitor, and a platelet aggregation inhibitor. Edoxaban tosylate monohydrate was developed by Daiichi Sankyo and approved in Japan in 2011. The systematic name (CAS Registry number 1229194-11-9) is *N*-(5-chloropyridin-2-yl)-*N*′-((1*S*,2*R*,4*S*)-4-(*N*,*N*-dimethylcarbamoyl)-2-(5-methyl-4,5,6,7-tetrahydrothiazolo(5,4-*c*)pyridine-2-carboxamido)cyclohexyl) ethanediamide *p*-toluenesulfonate monohydrate. The molecular structure of edoxaban tosylate monohydrate is illustrated in Figure 1.

Edoxaban was first claimed in US Patent 7,365,205 (Ohta *et al.*, 2008). European Patent Applications EP1405852 A1 (Ohta *et al.*, 2004) and EP 2371830 A1 (Koyama, 2011), as well as US Patent Application US 2017/0022220 A1 (Kawanami and Kitani, 2017), among others, disclose processes for the preparation of edoxaban tosylate monohydrate, but no powder diffraction data are provided. Canadian Patent Application CA 2793413 (Suzuki and Ono, 2011) reported powder patterns for both Form I and Form II of edoxaban tosylate monohydrate. European Patent Application EP 3318568 A1 (Berenguer Maimó *et al.*, 2018) claims a process for preparing edoxaban tosylate monohydrate and included a high-quality powder pattern of "edoxaban tosylate monohydrate reference standard" used for characterizing the products of the invention.

This work was carried out as part of a project (Kaduk *et al.*, 2014) to determine the crystal structures of large-volume commercial pharmaceuticals and include high-quality powder diffraction data for these pharmaceuticals in the Powder Diffraction File (Gates-Rector and Blanton, 2019).

II. EXPERIMENTAL

The sample was a commercial reagent, purchased from Sigma (Lot #A100306-001), and was used as-received. The white powder was packed into a 1.5-mm diameter Kapton capillary and rotated during the measurement at ~50 Hz. The powder pattern was measured at 295 K at beamline 11-BM (Lee *et al.*, 2008; Wang *et al.*, 2008) of the Advanced Photon Source at Argonne National Laboratory using a wavelength of 0.457899 Å from 0.5° to 50° 2θ with a step size of 0.001° and a counting time of 0.1 s step^{-1}.

The pattern was indexed on a primitive monoclinic unit cell with $a = 7.5521$, $b = 7.0904$, $c = 32.8086$ Å, $\beta = 94.26°$, $V = 1745.06$ Å^3, and $Z = 2$ using DICVOL14 (Louër and Boultif, 2014) through the PreDICT interface (Blanton *et al.*, 2019). Analysis of the systematic absences using EXPO2014 (Altomare *et al.*, 2013) suggested the space group $P2_1$, which was confirmed by successful solution and refinement of the structure. A reduced cell search in the Cambridge Structural Database (Groom *et al.*, 2016) yielded 3 hits, but no structures for edoxaban derivatives.

An edoxaban molecule was downloaded from PubChem as ConformerD_CID_10280735.sdf. It was converted to a .

a)Author to whom correspondence should be addressed. Electronic mail: kaduk@polycrystallography.com

 © 2021 JCPDS-ICDD
https://doi.org/10.1017/S0885715621000117 Published online by Cambridge University Press

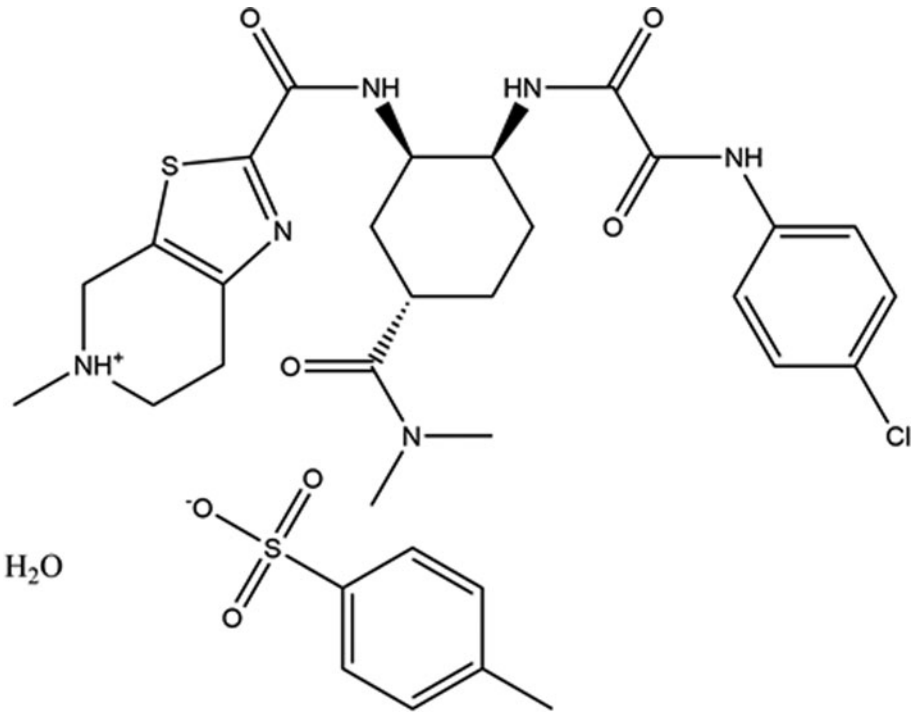

Figure 1. Two-dimensional diagram of the molecular structure of edoxaban tosylate monohydrate.

mol2 file using Materials Studio (Dassault, 2020), and converted into a Fenske-Hall *Z*-matrix using OpenBabel (O'Boyle *et al.*, 2011). A *p*-toluenesulfonate anion was built using Spartan '18 (Wavefunction, 2020), saved as a .mol2 file, and converted to a Fenske-Hall *Z*-matrix using the same tools. The structure was solved by Monte Carlo simulated annealing techniques as implemented in DASH (David *et al.*, 2006). An edoxaban molecule, a tosylate, and an O atom (water molecule) were used as fragments. A 001 preferred orientation coefficient was also included.

Rietveld refinement was carried out using GSAS-II (Toby and Von Dreele, 2013). Only the 0.5–25.0° portion of the pattern was included in the refinement ($d_{min} = 1.057$ Å). All non-H bond distances and angles were subjected to restraints, based on a Mercury/Mogul Geometry Check (Bruno *et al.*, 2004; Sykes *et al.*, 2011) of the model. The Mogul average and standard deviation for each quantity were used as the restraint parameters. The restraints contributed 7.6% to the final χ^2. The *y*-coordinate of Cl1 was fixed to define the origin. The hydrogen atoms were included in calculated positions, which were recalculated during the refinement using Materials Studio (Dassault, 2020). The U_{iso} were grouped by chemical similarity. The U_{iso} of the hydrogen atoms were constrained to be 1.3× that of the heavy atoms to which there are attached. The background was modeled using a 6-term shifted Chebyshev polynomial, along with two peaks at 1.71° and 5.89° to model the scattering from the Kapton capillary and any amorphous component of the sample. The peak profiles were described using the generalized microstrain model, and a second-order spherical harmonic preferred orientation model was included. N10···O80 was the only N···A distance < 3.2 Å, so we assumed that N10 was protonated, and added the remaining hydrogen atom there.

The final refinement of 186 variables using 25 340 observations and 124 restraints yielded the residuals $R_{wp} = 0.0826$ and GOF = 1.52. The largest peak (1.73 Å from C28) and hole (1.63 Å from C35) in the difference Fourier map were 0.51 and −0.43(11) eÅ^{-3}, respectively. The largest errors in the fit (Figure 2) are in the positions and shapes of some of the low-angle peaks, and may indicate subtle changes in the beam during the measurement.

A density functional geometry optimization (fixed experimental unit cell) was carried using CRYSTAL14 (Dovesi *et al.*, 2014). The basis sets for the H, C, N, and O atoms were those of Gatti *et al.* (1994), and those for Cl and S were those of Peintinger *et al.* (2013). The calculation was run on eight 2.1 GHz Xeon cores (each with 6 GB RAM) of a 304-core Dell Linux cluster at IIT, using 8 *k*-points and the B3LYP functional, and took ∼102 h.

III. RESULTS AND DISCUSSION

The synchrotron pattern from this study (Figure 3) of edoxaban tosylate monohydrate matches those of Berenguer Maimó *et al.* (2018) and Suzuki and Ono (2011) well enough to conclude that the material studied here is indeed Form I. The refined atom coordinates of edoxaban tosylate monohydrate Form I and the coordinates from the density functional theory (DFT) optimization are reported in the CIFs deposited with ICDD.

The root-mean-square (rms) Cartesian displacement of the non-hydrogen atoms in the Rietveld-refined and DFT-optimized structures is 0.196 Å (Figure 4), within the normal range for correct structures (van de Streek and Neumann, 2014). The maximum difference is 0.685 Å, at N10, and reflects a difference in the conformation of the tetrahydropyridine ring. The conformation difference will be discussed below. This discussion concentrates on the DFT-optimized structure, as we believe it is more reliable.

https://doi.org/10.1017/S0885715621000117 Published online by Cambridge University Press

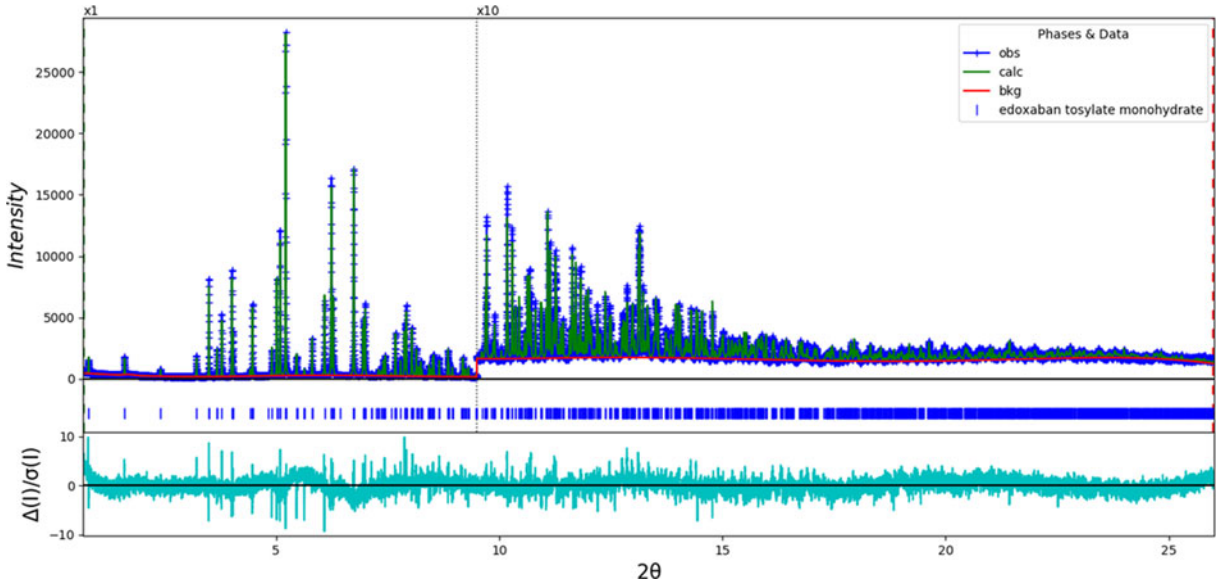

Figure 2. The Rietveld plot for the refinement of edoxaban tosylate monohydrate. The blue crosses represent the observed data points, and the green line is the calculated pattern. The cyan curve is the normalized error plot. The vertical scale has been multiplied by a factor of 10× for $2\theta > 9.5°$.

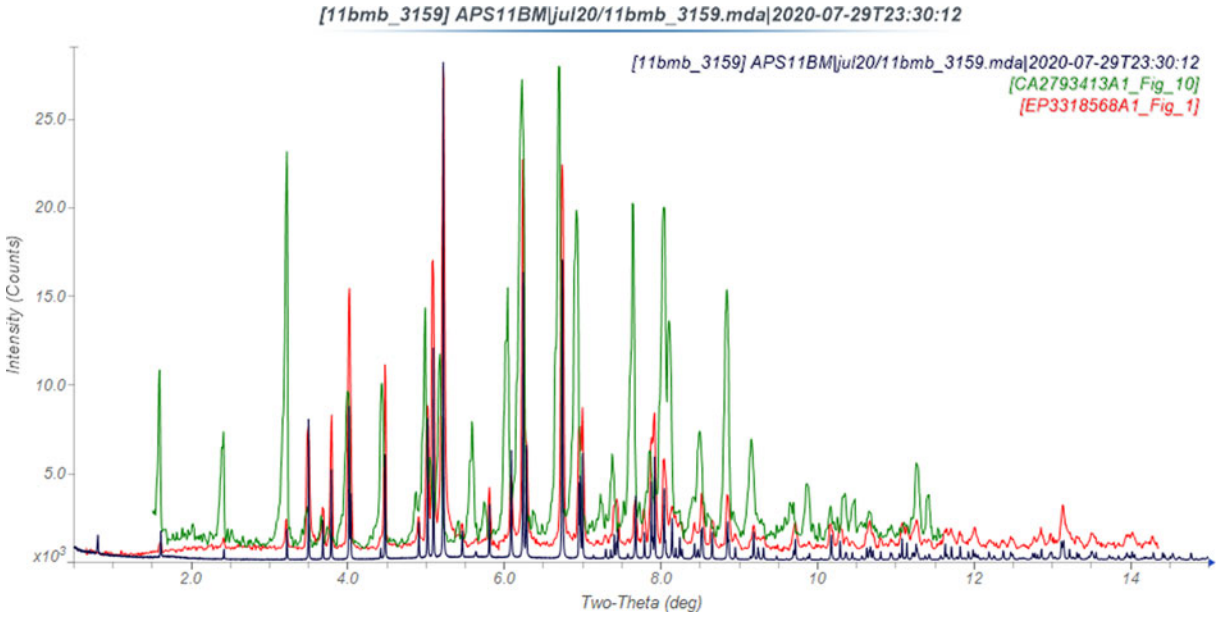

Figure 3. Comparison of the synchrotron pattern from this study (black) of edoxaban tosylate monohydrate to the patterns of form I reported by Berenguer Maimó *et al.* (2018) (red) and Suzuki and Ono (2011) (green). The published patterns were digitized using UN-SCAN-IT (Silk Scientific, 2013) and scaled to the synchrotron wavelength of 0.457899 Å using MDI JADE Pro (MDI, 2020).

The asymmetric unit (with atom numbering) is illustrated in Figure 5, and the crystal structure is presented in Figure 6.

The crystal structure consists of alternating layers of edoxaban cations and tosylate anions along the *c*-axis (Figure 6). The water molecules lie near the sulfonate end of the tosylate anions. The phenyl rings of the tosylates and the chloropyridine rings lie near each other.

Almost all of the bond distances, angles, and torsion angles fall within the normal ranges indicated by a Mercury/Mogul Geometry check (Macrae *et al.*, 2020). The C27–S2–C23 (87.2°, average = 91.4(4)°, *Z*-score = 9.2), C30–N10–C29 (119.1°, average = 111.5(19)°, *Z*-score = 3.8), and C29–C27–S2 (127.2°, average = 121.7(10)°, *Z*-score = 5.3) angles are flagged as unusual. The standard uncertainties on these averages are fairly small, but the differences may represent a weakness in the calculation of the environment around S2. The N10–C29–C27–C26–C28–C30 ring is flagged as unusual in the DFT-optimized structure, but not in the Rietveld-refined structure.

Quantum chemical geometry optimization of the edoxaban cation (DFT/B3LYP/6-31G*/water) using Spartan '18 (Wavefunction, 2020) indicated that the local minimum of the DFT configuration is only 0.6 kcal mol^{-1} lower in energy than that of the Rietveld configuration, even though the rms

https://doi.org/10.1017/S0885715621000117 Published online by Cambridge University Press

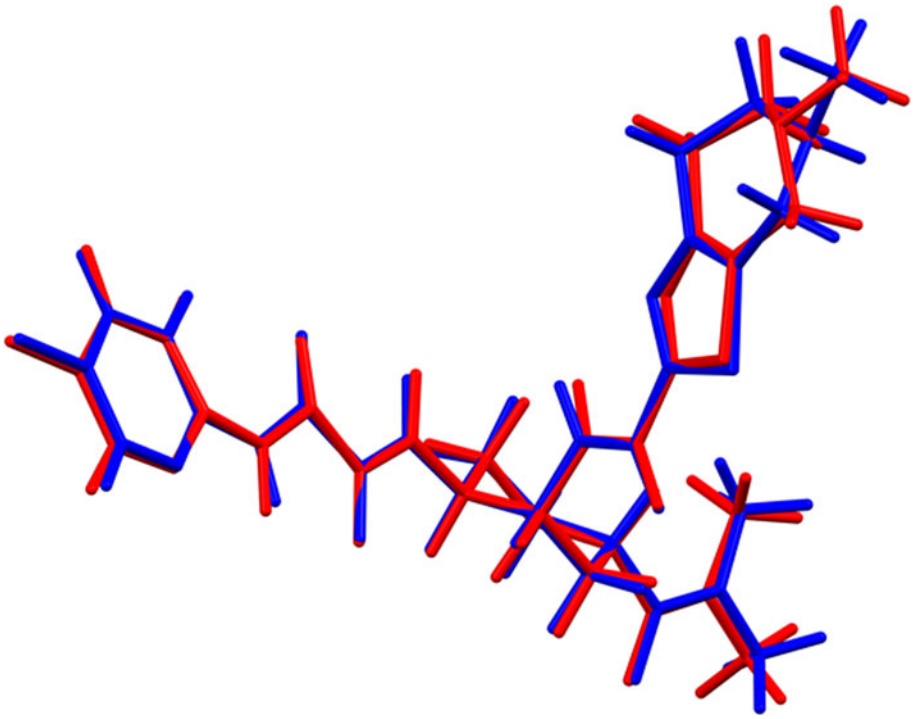

Figure 4. Comparison of the Rietveld-refined (red) and VASP-optimized (blue) structures of the edoxaban cation in edoxaban tosylate monohydrate. The rms Cartesian displacement of the cations is 0.196-Å.

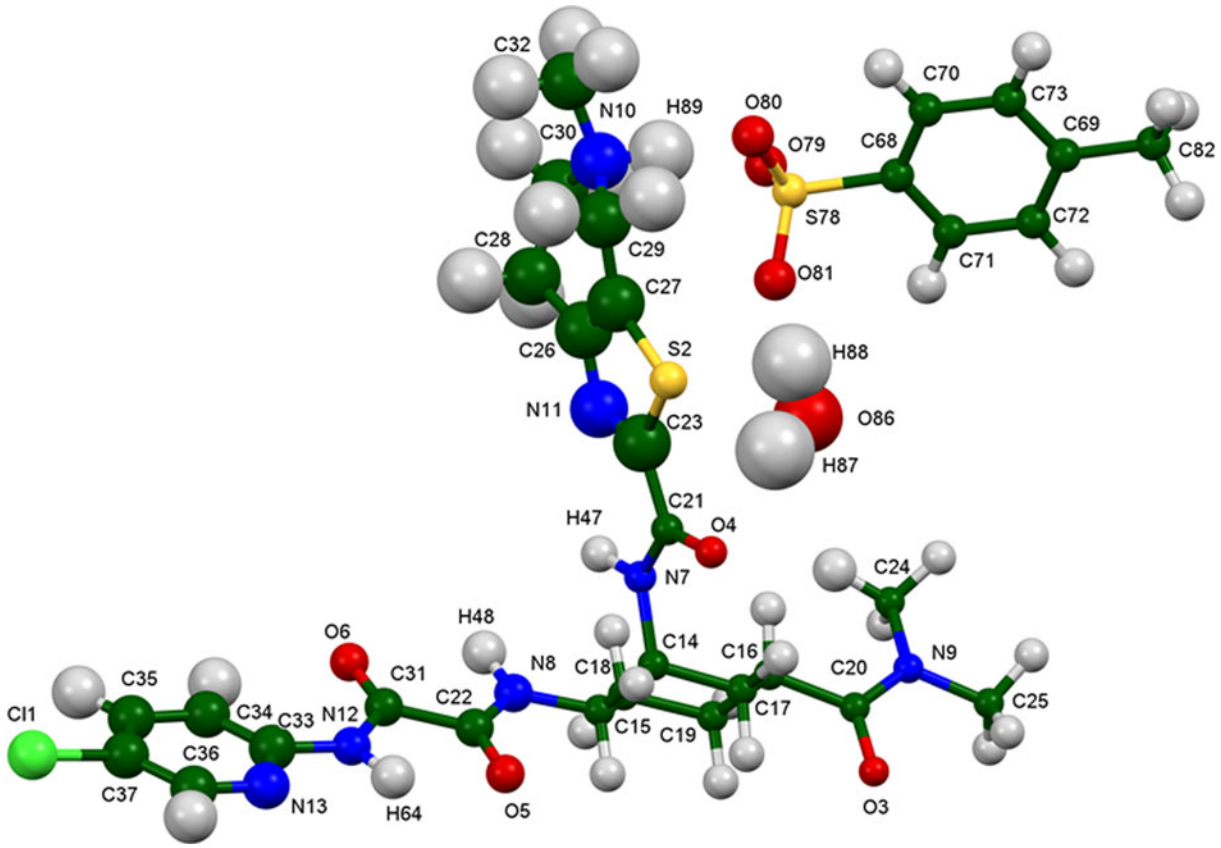

Figure 5. The asymmetric unit of edoxaban tosylate monohydrate Form I, with the atom numbering. The atoms are represented by 50% probability spheroids.

Cartesian displacement is 0.638 Å (Figure 7). The two conformations are, thus, equivalent in energy. The largest differences are in the conformation of the tetrahydropyridine ring at N10. The DFT conformation leads to a much more reasonable hydrogen-bonding geometry, so it is tempting to conclude that the solid-state interactions determine the

https://doi.org/10.1017/S0885715621000117 Published online by Cambridge University Press

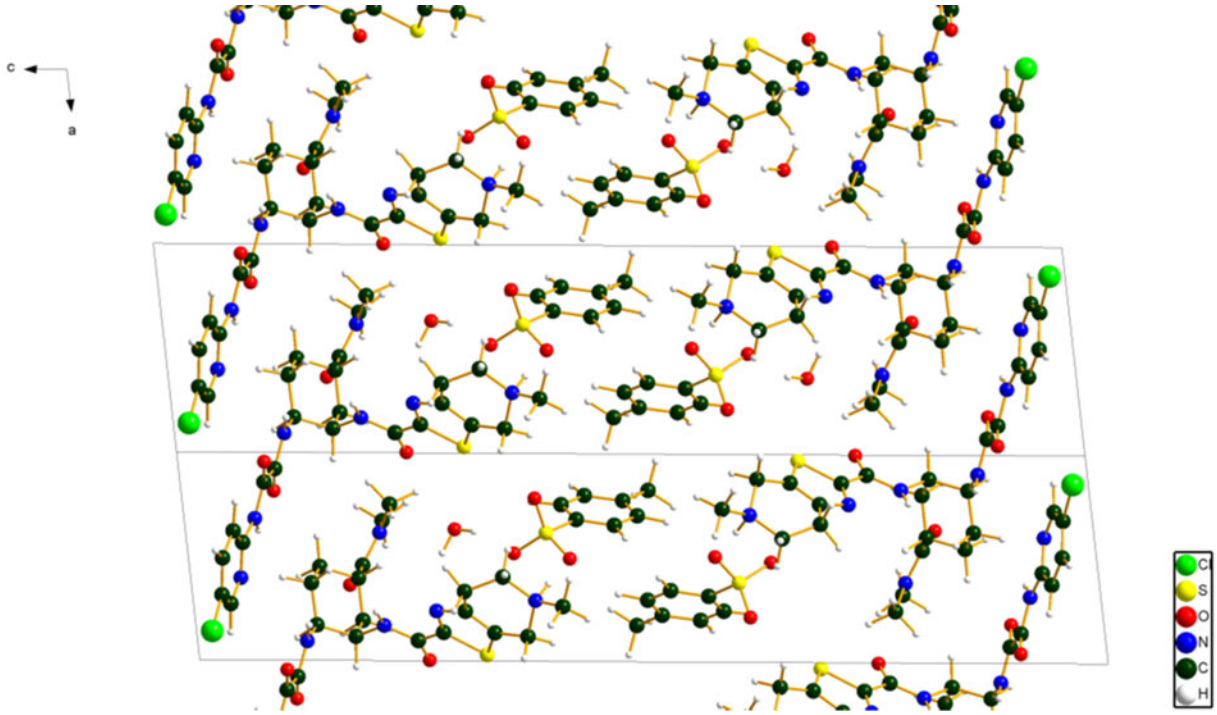

Figure 6. The DFT-optimized crystal structure of edoxaban tosylate monohydrate Form I, viewed down the *b*-axis.

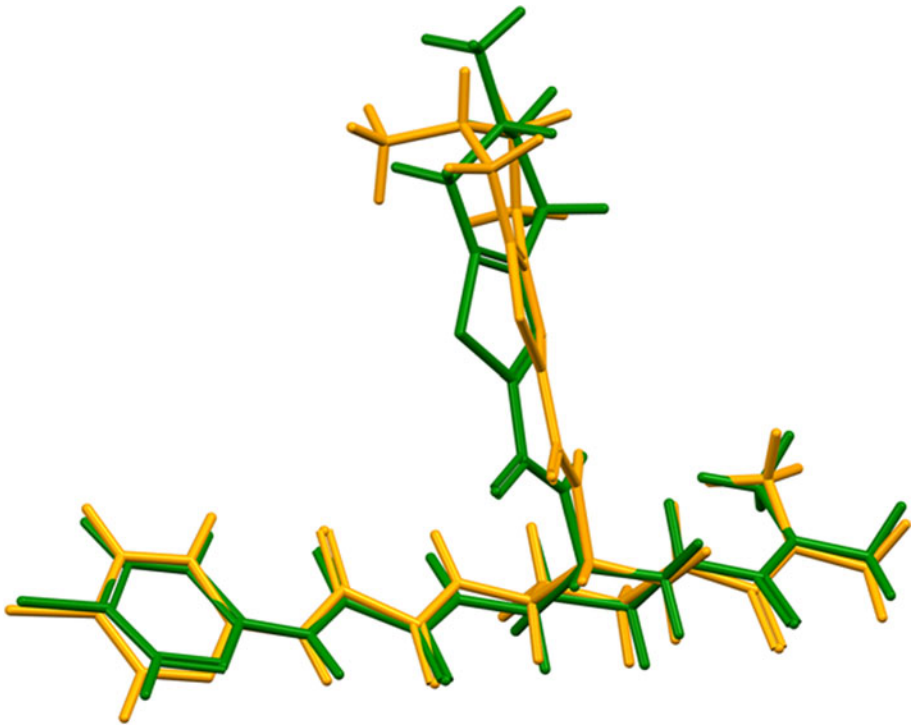

Figure 7. Comparison of the local minimum-energy conformations for the Rietveld-refined cation (orange) and the DFT-optimized cation (green) in edoxaban tosylate monohydrate.

conformation of the edoxaban cation. Molecular mechanics conformational analysis indicated that the global minimum-energy conformation is much more compact than the observed one, confirming that intermolecular ring–ring interactions are important to determining the observed conformation.

Analysis of the contributions to the total crystal energy using the Forcite module of Materials Studio (Dassault, 2020) suggests that angle deformation terms are the dominant contributions to the intramolecular deformation energy. The intermolecular energy is dominated by electrostatic repulsions (which in this force-field-based analysis include hydrogen

https://doi.org/10.1017/S0885715621000117 Published online by Cambridge University Press

TABLE I. Hydrogen bonds (CRYSTAL14) in edoxaban tosylate monohydrate.

H-Bond	D-H (Å)	H···A (Å)	D···A (Å)	D-H···A (°)	Overlap (*e*)	*E* (kcal mol^{-1})
N10–H89···O80	1.057	1.591	2.646	17.8	0.087	6.8
O86–H88···O81	0.976	1.854	2.766	154.4	0.042	11.2
O86–H87						
C73–H77···O80	1.084	2.207	3.206	152.1	0.029	
C72–H76···O79	1.085	2.335	3.309	148.3	0.022	
C30–H60···O81	1.087	2.405	3.466	164.9	0.020	
C30–H59···O79	1.091	2.857	3.877	155.6	0.011	
C29–H57···O79	1.089	2.384	2.979	112.7	0.011	
N12–H64···O5	1.017	2.058*	2.606	111.3	0.037	4.4
N7–H457···O3	1.024	1.979	2.984	166.3	0.047	5.0
N8–H48···O3	1.018	2.184	2.964	132.1	0.028	3.9
N8–H48···O6	1.018	2.415*	2.783	100.3	0.016	2.9
C36–H67···Cl1	1.082	2.678	3.608	143.8	0.013	
C25–H54···S2	1.088	2.921	4.004	173.8	0.021	
C36–H67···O6	1.082	2.447	3.166	122.7	0.012	
C34–G65···O5	1.017	2.363	3.227	114.2	0.015	
C28–H55···O4	1.095	2.250	3.318	164.6	0.028	
C18–H44···O3	1.092	2.258	3.149	137.3	0.019	
C17–H42···O6	1.094	2.531	3.574	159.0	0.014	
C17–H42···O3	1.094	2.468*	2.775	94.4	0.010	

*indicates intramolecular.

bonds) and van der Waals attractions. The hydrogen bonds are better analyzed using the results of the DFT calculation.

Hydrogen bonds are significant in the crystal structure (Table I). As expected, the protonated nitrogen atom N10 forms a strong N–H···O hydrogen bond to one of the tosylate oxygens. The energy was calculated using the correlation of Wheatley and Kaduk (2019). Only one of the water molecule hydrogens acts as a donor in an O–H···O hydrogen bond. The energy was calculated using the correlation of Rammohan and Kaduk (2018). The tosylate oxygens act as acceptors in a number of C–H···O hydrogen bonds. The amide nitrogens N12 and N7 act as donors to carbonyl oxygens, and the amino nitrogen N8 forms bifurcated hydrogen bonds to two carbonyl oxygens, one intra- and the other intermolecular. The chlorine Cl1 and sulfur S2 both act as acceptors in C–H···A hydrogen bonds. There are also several C–H···O hydrogen bonds to the carbonyl oxygens.

The volume enclosed by the Hirshfeld surface (Figure 8; Hirshfeld, 1977; Turner *et al.*, 2017) is 860.02 Å^3, 98.60% of half the unit cell volume. The molecules are, thus, not tightly packed. All of the significant-close contacts (red in Figure 8) involve the hydrogen bonds. The volume/non-hydrogen atom is 17.8 Å^3.

The Bravais–Friedel–Donnay–Harker (Bravais, 1866; Friedel, 1907; Donnay and Harker, 1937) morphology suggests that we might expect platy morphology for edoxaban tosylate monohydrate, with {001} as the principal faces. A second-order spherical harmonic model for preferred

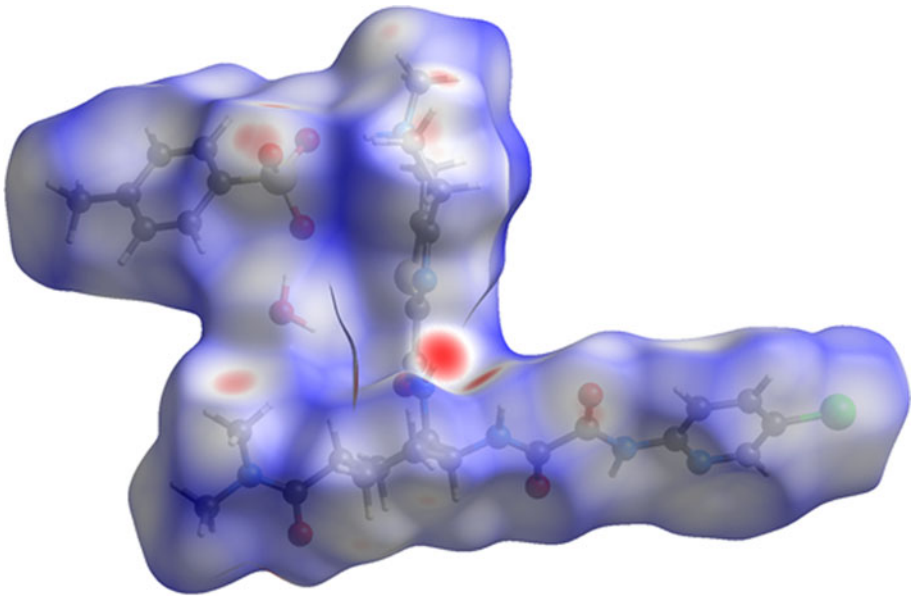

Figure 8. The Hirshfeld surface of edoxaban tosylate monohydrate. Intermolecular contacts longer than the sums of the van der Waals radii are colored blue, and contacts shorter than the sums of the radii are colored red. Contacts equal to the sums of radii are white.

https://doi.org/10.1017/S0885715621000117 Published online by Cambridge University Press

orientation was incorporated into the refinement. The texture index was only 1.023(0), indicating that preferred orientation was slight in this rotated capillary specimen. The powder pattern of edoxaban tosylate monohydrate from this synchrotron data set has been submitted to ICDD for inclusion in the Powder Diffraction File.

IV. DEPOSITED DATA

The Crystallographic Information Framework (CIF) files containing the results of the Rietveld refinement (including the raw data) and the DFT geometry optimization were deposited with the ICDD. The data can be requested at info@icdd.com.

ACKNOWLEDGEMENTS

Use of the Advanced Photon Source at Argonne National Laboratory was supported by the U.S. Department of Energy, Office of Science, Office of Basic Energy Sciences, under Contract No. DE-AC02-06CH11357. This work was partially supported by the International Centre for Diffraction Data. We thank Lynn Ribaud and Saul Lapidus for their assistance in the data collection, and Andrey Rogachev for the use of computing resources at IIT.

CONFLICTS OF INTEREST

The authors have no conflicts of interest to declare.

Altomare, A., Cuocci, C., Giacovazzo, C., Moliterni, A., Rizzi, R., Corriero, N., and Falcicchio, A. (**2013**). "EXPO2013: a kit of tools for phasing crystal structures from powder data," J. Appl. Crystallogr. **46**, 1231–1235.

Berenguer Maimó, R., Racamonde Villanueva, M., and Winter, S. B. D. (**2018**). "Preparation process of edoxaban tosylate monohydrate," European Patent Application EP3318568.

Blanton, J. R., Papoular, R. J., and Louër, D. (**2019**). "PreDICT: a graphical user interface to the DICVOL14 indexing software program for powder diffraction data," Powder Diffr. **34**, 233–241.

Bravais, A. (**1866**). *Etudes Cristallographiques* (Gauthier Villars, Paris).

Bruno, I. J., Cole, J. C., Kessler, M., Luo, J., Motherwell, W. D. S., Purkis, L. H., Smith, B. R., Taylor, R., Cooper, R. I., Harris, S. E., and Orpen, A. G. (**2004**). "Retrieval of crystallographically-derived molecular geometry information," J. Chem. Inf. Sci. **44**, 2133–2144.

Dassault Systèmes (**2020**). *Materials Studio 2020* (BIOVIA, San Diego, CA).

David, W. I. F., Shankland, K., van de Streek, J., Pidcock, E., Motherwell, W. D. S., and Cole, J. C. (**2006**). "DASH: a program for crystal structure determination from powder diffraction data," J. Appl. Crystallogr. **39**, 910–915.

Donnay, J. D. H. and Harker, D. (**1937**). "A new law of crystal morphology extending the law of bravais," Am. Mineral. **22**, 446–447.

Dovesi, R., Orlando, R., Erba, A., Zicovich-Wilson, C. M., Civalleri, B., Casassa, S., Maschio, L., Ferrabone, M., De La Pierre, M., D-Arco, P., Noël, Y., Causà, M., and Kirtman, B. (**2014**). "CRYSTAL14: a program for the ab initio investigation of crystalline solids," Int. J. Quantum Chem. **114**, 1287–1317.

Friedel, G. (**1907**). "Etudes sur la loi de bravais," Bull. Soc. Fr. Mineral. **30**, 326–455.

Gates-Rector, S. and Blanton, T. (**2019**). "The Powder Diffraction File: a quality materials characterization database," Powder Diffr. **39**, 352–360.

Gatti, C., Saunders, V. R., and Roetti, C. (**1994**). "Crystal-field effects on the topological properties of the electron-density in molecular crystals - the case of urea," J. Chem. Phys. **101**, 10686–10696.

Groom, C. R., Bruno, I. J., Lightfoot, M. P., and Ward, S. C. (**2016**). "The Cambridge structural database," Acta Crystallogr. Sect. B: Struct. Sci., Cryst. Eng. Mater. **72**, 171–179.

Hirshfeld, F. L. (**1977**). "Bonded-atom fragments for describing molecular charge densities," Theor. Chem. Acta **44**, 129–138.

Kaduk, J. A., Crowder, C. E., Zhong, K., Fawcett, T. G., and Suchomel, M. R. (**2014**). "Crystal structure of atomoxetine hydrochloride (Strattera), $C_{17}H_{22}NOCl$," Powder Diffr. **29**, 269–273.

Kawanami, K. and Kitani, Y. (**2017**). "High-purity crystals of active blood coagulation factor X (FXA) inhibitor," US Patent Application 2017/0022220 A1.

Koyama, T. (**2011**). "Method for producing diamine derivatives," European Patent Application EP2371830A1.

Lee, P. L., Shu, D., Ramanathan, M., Preissner, C., Wang, J., Beno, M. A., Von Dreele, R. B., Ribaud, L., Kurtz, C., Antao, S. M., Jiao, X., and Toby, B. H. (**2008**). "A twelve-analyzer detector system for high-resolution powder diffraction," J. Synchroton Radiat. **15**, 427–432.

Louër, D. and Boultif, A. (**2014**). "Some further considerations in Powder Diffraction Pattern indexing with the dichotomy method," Powder Diffr. **29**, S7–S12.

Macrae, C. F., Sovago, I., Cottrell, S. J., Galek, P. T. A., McCabe, P., Pidcock, E., Platings, M., Shields, G. P., Stevens, J. S., Towler, M., and Wood, P. A. (**2020**). "*Mercury 4.0*; from visualization to design and prediction," J. Appl. Crystallogr. **53**, 226–235.

MDI (**2020**). *JADE Pro version 7.8* (Computer software), Materials Data, Livermore, CA, USA.

O'Boyle, N., Banck, M., James, C. A., Morley, C., Vandermeersch, T., and Hutchison, G. R. (**2011**). "Open babel: an open chemical toolbox," J. Chem. Informatics **3**, 33. doi:10.1186/1758-2946-3-33.

Ohta, T., Komoriya, S., Yoshino, T., Uoto, K., Nakamoto, Y., Naito, H., Mochizuki, A., Nagata, T., Kanno, H., Haginoya, N., Yoshikawa, K., Nagamochi, M., Kobayashi, S., and Ono, M. (**2004**). "Diamine derivatives," European Patent Application EP1405852A1.

Ohta, T., Komoriya, S., Yoshino, T., Nagamochi, M., and Ono, M. (**2008**). "Diamine derivatives," US Patent 7,365,205 B2.

Peintinger, M. F., Vilela Oliveira, D., and Bredow, T. (**2013**). "Consistent Gaussian basis sets of triple-Zeta valence with polarization quality for solid-state calculations," J. Comput. Chem. **34**, 451–459.

Rammohan, A. and Kaduk, J. A. (**2018**). "Crystal structures of alkali metal (group 1) citrate salts," Acta Crystallogr. Sect. B: Struct. Sci., Cryst. Eng. Mater. **74**, 239–252. doi:10.1107/S2052520618002330.

Silk Scientific (**2013**). *UN-SCAN-IT 7.0* (Silk Scientific Corporation, Orem, UT).

Suzuki, T. and Ono, M. (**2011**). "Crystal of diamine derivative and method of producing same," Canadian Patent Application CA2793413.

Sykes, R. A., McCabe, P., Allen, F. H., Battle, G. M., Bruno, I. J., and Wood, P. A. (**2011**). "New software for statistical analysis of Cambridge Structural Database data," J. Appl. Crystallogr. **44**, 882–886.

Toby, B. H. and Von Dreele, R. B. (**2013**). "GSAS II: the genesis of a modern open source all purpose crystallography software package," J. Appl. Crystallogr. **46**, 544–549.

Turner, M. J., McKinnon, J. J., Wolff, S. K., Grimwood, D. J., Spackman, P. R., Jayatilaka, D., and Spackman, M. A. (**2017**). *CrystalExplorer17* (University of Western Australia). Available at: http://hirshfeldsurface.net.

van de Streek, J. and Neumann, M. A. (**2014**). "Validation of molecular crystal structures from powder diffraction data with dispersion-corrected density functional theory (DFT-D)," Acta Crystallogr. Sect. B: Struct. Sci., Cryst. Eng. Mater. **70**, 1020–1032.

Wang, J., Toby, B. H., Lee, P. L., Ribaud, L., Antao, S. M., Kurtz, C., Ramanathan, M., Von Dreele, R. B., and Beno, M. A. (**2008**). "A dedicated powder diffraction beamline at the advanced photon source: commissioning and early operational results," Rev. Sci. Instrum. **79**, 085105.

Wavefunction, Inc. (**2020**). Spartan '18 Version 1.4.0, Wavefunction Inc., 18401 Von Karman Ave., Suite 370, Irvine, CA 92612.

Wheatley, A. M. and Kaduk, J. A. (**2019**). "Crystal structures of ammonium citrates," Powder Diffr. **34**, 35–43.

https://doi.org/10.1017/S0885715621000117 Published online by Cambridge University Press